Received: 5 September 2018 | Revised: 8 November 2018 | Accepted: 27 November 2018

DOI: 10.1002/jmr.2775

RESEARCH ARTICLE

WILEY Journal of Molecular Recognition

Modification of nanocrystalline TiO_2 coatings with molecularly imprinted TiO_2 for uric acid recognition

Chunlei Zhang[1] | Zhiguo Xiao[2] | Tongtong Qin[3] | Zhengpeng Yang[3]

[1] Bone Tumour and Bone Disease Department II, Zhengzhou Orthopaedic Hospital, Zhengzhou, China

[2] College of Safety Science and Engineering, Henan Polytechnic University, Jiaozuo, China

[3] Institute of Materials Science and Engineering, Henan Polytechnic University, Jiaozuo, China

Correspondence
Zhiguo Xiao, College of Safety Science and Engineering, Henan Polytechnic University, Jiaozuo 454000, China.
Email: zgxiao2020@163.com

Zhengpeng Yang, Institute of Materials Science and Engineering, Henan Polytechnic University,Jiaozuo 454000, China.
Email: zhengpengyang2013@163.com

Funding information
Doctoral Foundation Henan Polytechnic University, China, Grant/Award Number: B2016-08; Key Foundation of Henan Educational Committee, Grant/Award Number: 18A150029; Natural Science Foundation of Henan Province of China, Grant/Award Numbers: 182300410201 and 182300410202; Program for Science Technology Innovation Talents in Universities of Henan Province, Grant/Award Number: 18HASTIT007; Key Research Project of Henan Province, Grant/Award Number: 162102210223

Abstract

Combining the surface modification and molecular imprinting technique, a novel piezoelectric sensing platform with excellent molecular recognition capability was established for the detection of uric acid (UA) based on the immobilization of TiO_2 nanoparticles onto quartz crystal microbalance (QCM) electrode and modification of molecularly imprinted TiO_2 (MIT) layer on TiO_2 nanoparticles. The performance of the fabricated biosensor was evaluated, and the results indicated that the biosensor exhibited high sensitivity in UA detection, with a linear range from 0.04 to 45 μM and a limit of detection of 0.01 μM. Moreover, the biosensor presented high selectivity towards UA in comparison with other interferents. The analytical application of the UA biosensor confirmed the feasibility of UA detection in urine sample.

KEYWORDS

highly selective detection, molecularly imprinted TiO_2, piezoelectric sensing, surface modification, uric acid biosensor

1 | INTRODUCTION

Uric acid (UA), a primary final product of purine metabolism, is found in urine, saliva, blood serum, and plasma.[1] UA detection is clinically important because of its association with several diseases such as gout, hypertension, Lesch-Nyhan syndrome, hyperuricemia, pneumonia, cardiovascular, and leukemia.[1,2] Recently, the low UA level in the serum and/or cerebrospinal fluid has been proved to be a key biomarker of Parkinson disease.[3] In the past years, some analytical methods have been developed for UA detection, including high-performance liquid chromatography (HPLC),[4] chemiluminescence,[5] electrochemistry,[6-8] enzymatic assay,[9,10] fluorescence,[11,12] surface plasmon resonance,[3] and photoelectrochemistry.[11,12] Despite many advances in UA detection, many of these methods still do not meet the growing demand for more sensitive and selective detection of UA. Thus, the further development of stable and facile methods with high sensitivity and selectivity for UA detection is highly desirable.

The quartz crystal microbalance (QCM) is a simple, portable, cost-effective, high-resolution mass-sensing instrument, which has been favorably adopted for analytical application because of its extreme sensitivity to the nanogram level of mass change loaded onto surface of the QCM resonator.[13,14] As a mass sensor, QCM has been widely used in biochemistry, environment, food, life science, and clinical analysis because the instrument provides a label-less method for the direct study of biospecific interaction process.[15-17] Still, the QCM response lacks selectivity because of the nature of mass sensing, which will limit its application. Therefore, how to realize the selectivity of a QCM sensor is a quite critical issue. Molecular imprinting technique, the design and construction of mimetic receptor system with predetermined recognition for

target molecule, has been proposed and developed rapidly.[18-23] QCM sensors based on molecularly imprinted polymer (MIP) have been fabricated and exhibited a favorable selectivity towards template molecules.[24,25] Recently, inorganic matrices have been employed for molecular imprinting. Compared with MIP, molecularly imprinted inorganic matrices not only possessed a better stability and structural rigidity but also relieved some drawbacks of organic material such as low binding efficiency, slow binding process, and difficult fabrication.[26] Silica, hydroxyapatite, and TiO_2 sol-gel materials have been used to prepare molecularly imprinted thin films at the surface of QCM electrode, which were used for the detection of organisms.[27-29] Despite molecularly imprinted inorganic films exhibited favorable selectivity in piezoelectric sensing, the electrodes usually possessed a small surface to volume ratio, significantly affecting their sensing performance. It is expected that, if an imprinted inorganic layer on QCM electrode is highly rough, the surface area of electrode will be greatly elevated, facilitating adsorption of molecules or ions and improving the sensing performance for UA.

In this work, TiO_2 nanoparticles and MIT were employed as carrier and sensing layer, respectively. A novel QCM biosensor with molecular recognition capability has been developed for UA detection based on the immobilization of TiO_2 nanoparticles onto QCM electrode and modification of MIT layer on TiO_2 nanoparticles. The constructed QCM biosensor with high sensitivity, selectivity, and stability showed excellent performance for the detection of UA.

2 | EXPERIMENTAL SECTION

2.1 | Materials and apparatus

$Ti(O\text{-}^nBu)_4$ was purchased from Sigma Chem Co and used as received. TiO_2 nanoparticles with ca 100 nm of mean particle diameter were purchased from Aladdin Reagent Co. UA, ascorbic acid (AA), urea, glucose, glutamic acid (GA), purine, and cytosine were purchased from Shanghai Sinopharm Chemical Reagent Co, China. All other chemicals were of analytical grade, and deionized (DI) water was used throughout the experiments.

Piezoelectric measurements were performed using a Q-sense instrument (Gothenburg, Sweden). Mechanically polished AT-cut 9-MHz quartz crystals (diameter of 12 mm, Beijing Chenjing Co, Beijing, China) were vacuum deposited with gold electrodes (6-mm diameter) on both sides of the surface. To reduce background frequency drift, one electrode was completely insulated from the test liquid. This was accomplished by the method reported in our previous study.[30] The frequency was monitored by a frequency counter (Iwatsu, Model SC-7201), and the recorded data were stored in a computer. X-ray diffraction (XRD) was recorded on a Bruker-AXS D8 X-ray diffractometer system operating with a Cu-Kα radiation. Infrared spectra were recorded on Nicolet 200SXV Fourier-transform infrared (FTIR) spectrometer using a KBr wafer. Scanning electron micrograph (SEM) was conducted on a Hitachi S-520 scanning electron microscope (Hitachi Ltd, Tokyo, Japan) working at 20 kV.

2.2 | Design and fabrication of the UA biosensor

The TiO_2 nanoparticles were attached to the surface of QCM electrode according to the procedures reported in our previous study.[31] The TiO_2 coatings with 0.8 μm thickness were employed in our study, unless otherwise stated. The obtained coatings were finally heat-treated at 300°C for 1.5 hours and then used for MIT modification.

The formation of MIT layer on TiO_2 nanoparticle/QCM electrode was performed by sol-gel hydrolysis of $Ti(O\text{-}^nBu)_4$ followed by calcination treatment. Specifically, $Ti(O\text{-}^nBu)_4$ (0.8 mmol) and UA (0.3 mmol) were dissolved in 10 mL of toluene-ethanol (*v*/v, 2:1) mixture and then vigorously stirred at room temperature. Subsequently, the solution was diluted by 20 times with water-saturated toluene and continuously stirred for 6 hours to get a sol-gel solution, which was used as a dipping solution. The obtained TiO_2 nanoparticle/QCM electrode was immersed into the dipping solution for 8 minutes at room temperature, rinsed with toluene, hydrolyzed in water, and dried in N_2 atmosphere. The "dipping-rinse-hydrolyzation-drying" cycle was repeated three times, and then the TiO_2 nanoparticle/QCM electrode whose surface was covered with a TiO_2 layer containing the template molecule of UA was obtained. Finally, the TiO_2 nanoparticle/QCM electrode modified by TiO_2 layer was dried at 80°C for 2 hours and then calcined in air at 350°C for 3 hours to remove template molecules and crystalline the TiO_2, causing the formation of MIT/TiO_2 nanoparticle/QCM electrode. Thus, the UA biosensor was fabricated. For comparison, the formation of nonimprinted TiO_2 on TiO_2 nanoparticle/QCM electrode was carried out using a similar procedure without template molecules and was denoted as NIT/TiO_2 nanoparticle/QCM electrode.

2.3 | QCM measurements

The piezoelectric measurements of the obtained UA biosensor were performed at 25°C. After mounting the MIT/TiO_2 nanoparticle/QCM electrode in the cell, 20 mL of 0.01-mM phosphate buffer solution (PBS, pH 7.4) was introduced into the cell. When the frequency became stable, UA aqueous solution (1 mL) with various concentrations was injected into the detection system within 5 seconds. Time-dependent change in the frequency was recorded continuously by a frequency counter and stored in a microcomputer during the reaction process of UA.

3 | RESULTS AND DISCUSSION

3.1 | Fabrication and characterization of the UA biosensor

The route of design and fabrication of the UA biosensor was shown in Figure 1. The TiO_2 coatings were formed at the surface of QCM electrode using the aqueous suspensions of ca 100-nm diameter TiO_2 nanoparticles by spin coating. The MIT layer was functionalized on the TiO_2 nanoparticle modified QCM electrode by the sol-gel hydrolysis of $Ti(O\text{-}^nBu)_4$ in the presence of the template molecules UA. UA was embedded in TiO_2 layer by strong hydrogen bond formed

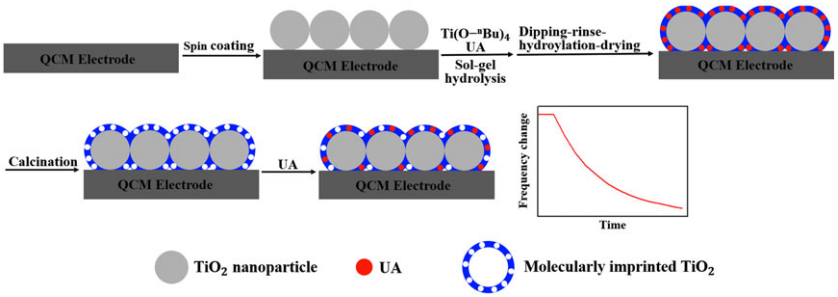

FIGURE 1 Schematic illustration for fabrication and detection mechanism of the UA biosensor

between N-H groups of UA and hydroxyl groups of TiO_2. After removal of UA, recognition sites complementary to the molecular shape, size, and functionality of UA were formed in TiO_2 layer, which would efficiently and selectively rebind UA in solution, causing a frequency change of QCM.

Corroborating evidence for the presence of MIT layer on the TiO_2 nanoparticle modified QCM electrode was provided by SEM studies. Figure 2 shows the surface morphologies of quartz crystal, TiO_2 layer, and MIT layer. Compared with bare surface of a QCM electrode (Figure 2A), the quartz crystal modified by TiO_2 nanoparticles was actually rather rough and was composed of closely packed nanometer-sized spherical grains, which were remarkably uniform with an average size of ca 100 nm in the diameter (Figure 2B). The MIT modification at the surface of TiO_2 nanoparticles attached to QCM electrode showed significant difference. As seen in Figure 2C, the electrode surface appeared to be completely covered by the MIT modification layer, which was homogeneous and free from appreciable cracks. From the enlarged SEM image (Figure 2D), the plentiful cavities were present in the MIT modification layer. These relative uniform cavities can be related to the removal of UA molecules in the process of MIT layer formation at the surface of a QCM electrode. SEM observation indicated the formation of MIT/TiO_2 nanoparticle modification layer on QCM electrode. The crystal structure and composition of electrode were identified by XRD and FTIR. As seen in Figure 3A, the relatively narrow diffraction peaks at 2θ = 25.4°, 37.9°, 48°, 54.6,° and 62.7 ° could be perfectly assigned to the typical crystal planes of anatase,[26] and the infrared spectrum also revealed the characteristic peaks of TiO_2 at 3410, 1657, and 900 to 400 cm^{-1} (Figure 3B).[31] Both XRD and FTIR analyses indicated the presence of anatase TiO_2 on the QCM electrode.

The formation of MIT layer on the TiO_2 nanoparticle/QCM electrode was further evaluated using piezoelectric measurements. Figure 4 shows the frequency responses with time on QCM electrode, NIT/TiO_2 nanoparticle/QCM electrode, and MIT/TiO_2 nanoparticle/QCM electrode in 10-μM UA solution. No obvious frequency response was found on the bare QCM electrode, while the larger frequency responses to the adsorption of UA were clearly observed on NIT/TiO_2 nanoparticle/QCM electrode and MIT/TiO_2 nanoparticle/QCM electrode. The frequency change on MIT/TiO_2 nanoparticle/QCM electrode reached 275 Hz, which was 3.3 times that on NIT/TiO_2 nanoparticle/QCM electrode. Significantly, the imprinted electrode exhibited much larger response compared with the nonimprinted electrode. The larger frequency change can be closely related to the presence of MIT layer on the electrode surface. The recognition sites situated in the MIT layer can specifically rebind and accumulate UA molecules on the electrode surface. As a result, more UA molecules were adsorbed on the imprinted electrode, causing a higher frequency change. The results demonstrated that the binding affinity of the imprinted electrode was due to the specific recognition sites formed in the imprinting process. Thus, the piezoelectric

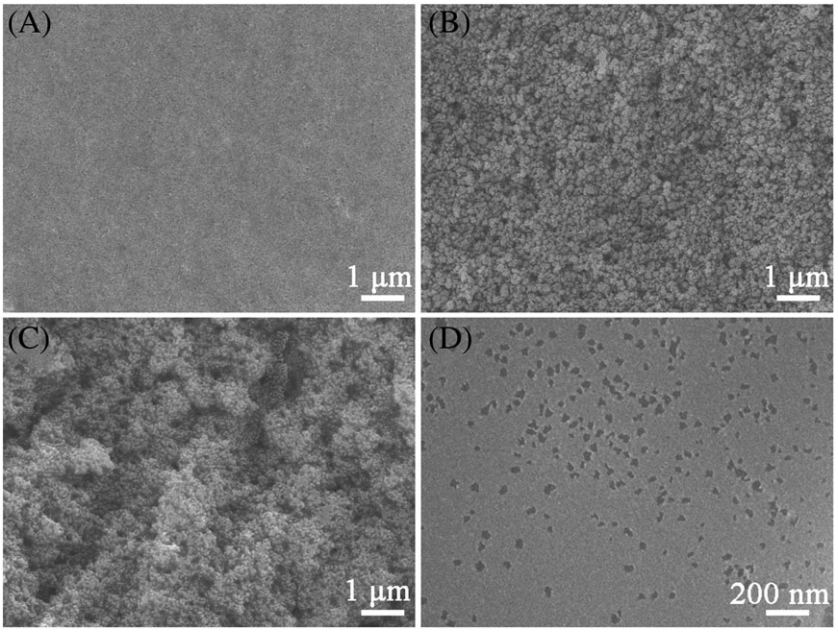

FIGURE 2 A, SEM micrographs of QCM electrode; B, TiO_2 nanoparticle/QCM electrode; C, MIT/TiO_2 nanoparticle/QCM electrode; and D, MIT modification layer at high magnification

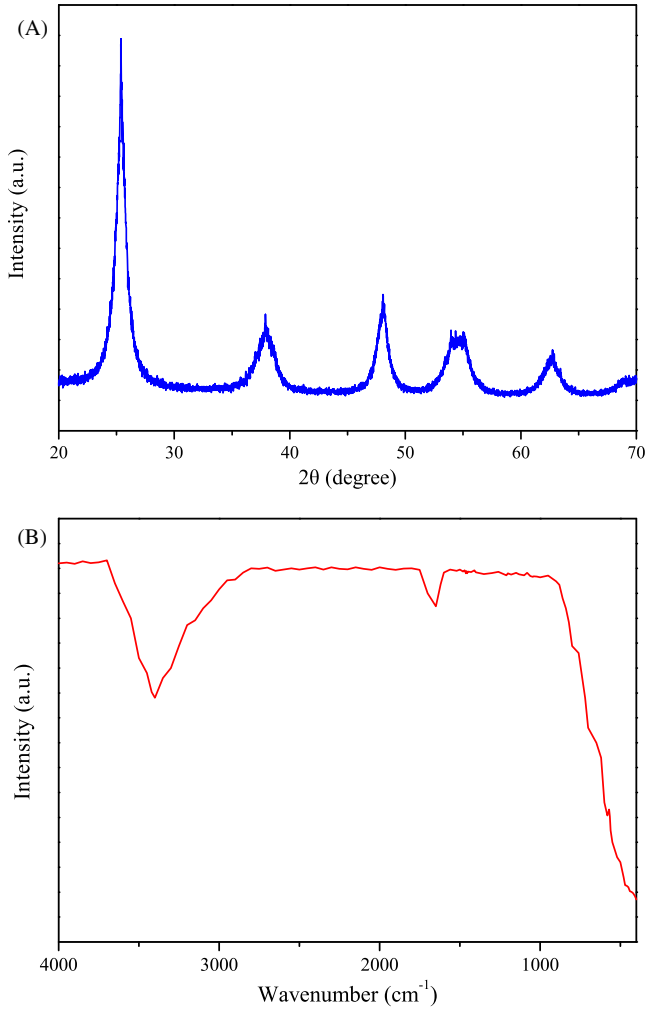

FIGURE 3 XRD pattern (A) and infrared spectrum (B) of MIT/TiO_2 nanoparticle modification layer on QCM electrode

measurements confirmed strongly the existence of MIT layer on the TiO_2 nanoparticle/QCM electrode surface. Furthermore, note that a steady-state response could be reached within ca 35 minutes.

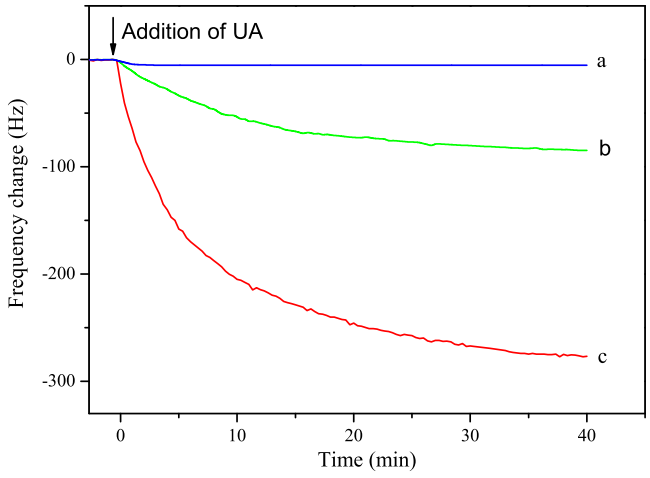

FIGURE 4 Frequency change of QCM after the addition of 10-μM UA solution (pH 7.4, 25°C) to the detector cell. A, QCM electrode; B, NIT/TiO_2 nanoparticle/QCM electrode; and C, MIT/TiO_2 nanoparticle/QCM electrode

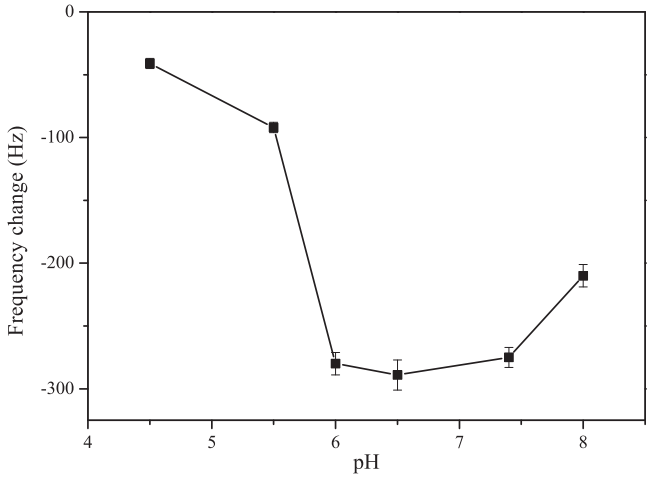

FIGURE 5 Effect of pH on frequency response of the UA biosensor; 10-μM UA, 25°C, average of three experiments

3.2 | Biosensing performance

The frequency response of UA biosensor as a function of pH was examined, and the obtained results were exhibited in Figure 5. The value in frequency change increased sharply when pH was varied from 4.5 to 6, kept a small change in the pH range of 6 to 7.4, and then

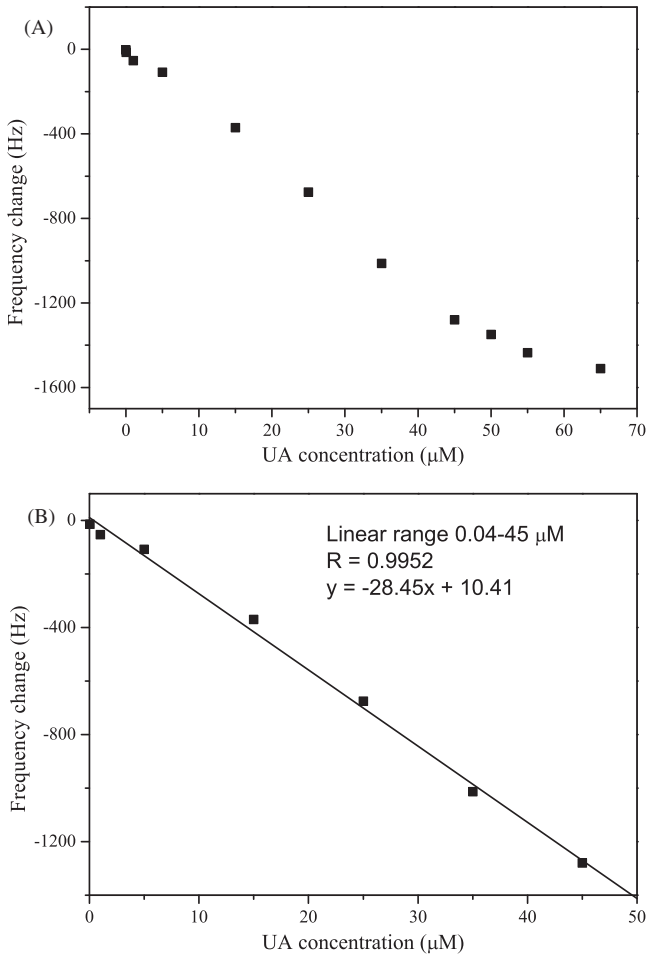

FIGURE 6 A, Calibration graph obtained for the UA biosensor in a UA concentration range from 0.01 to 65 μM. B, The linear part of the calibration graph. Experimental conditions: pH 7.4 and 25°C

TABLE 1 Comparison in performance of molecularly imprinted TiO_2/TiO_2-based uric acid (UA) sensor with other reported UA sensors

Sensing Materials	Methods	Linear Range, μM	Detection Limit, μM	Ref
HNP-PtTi	Electrochemistry	100-1000	5.3	7
PEI/[$P_2W_{16}V_2$-Au/	Electrochemistry	0.25-150	0.08	8
PDDA-rGO]$_n$				
Enzyme-UCNPs	Enzymatic assay	20-850	6.7	9
AUR-Co^{2+}	Fluorometry	0.05-1	0.02	11
G-quadruplex/	Fluorometry	2-300	0.5	12
Hemin DNAzyme				
Fe_3O_4@C@MIT	Photoelectrochemistry	0.3-34	0.02	13
ZnS urchin	Photoelectrochemistry	10-540	0.045	14
MIT/TiO_2	Piezoelectricity	0.04-45	0.01	This work

Abbreviations: AUR, Amplex UltraRed; G, graphene; HNP, hierarchical nanoporous; PDDA, poly(diallyldimethylammonium chloride); PEI, poly(ethylenimine); rGO, reduced graphene oxide; UCNPs, upconversion nanoparticles.

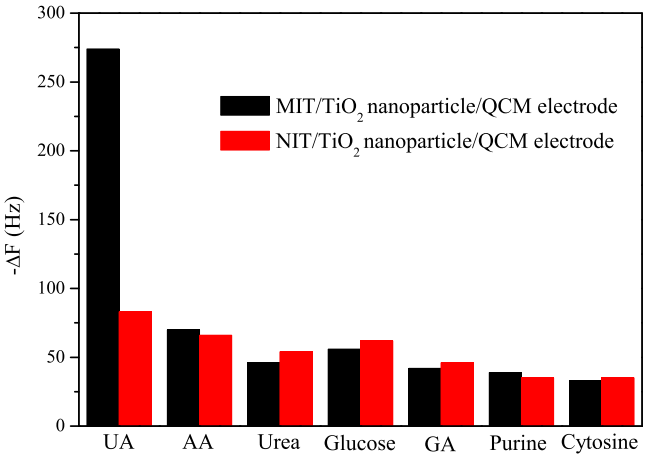

FIGURE 7 Comparison of adsorption selectivity of the QCM biosensors. Concentration 10.0 μM, pH 7.4, and temperature 25°C

decreased obviously at pH above 7.4. The isoelectric point (ca 6.8) of TiO_2[32] and pKa (5.4) of UA[33] are responsible for the frequency change with pH. The comparatively low frequency change at pH below 6 and above 7.4 can be attributed to the low solubility of UA and electrostatic repulsion respectively, inhibiting the UA adsorption, and the strong frequency response in the pH range of 6 to 7.4 can be due to the electrostatic attraction between TiO_2 and UA, enhancing the UA adsorption. Considering the physiological conditions, the optimum pH 7.4 was used in the following experiments.

The linear dynamic range of the UA biosensor was investigated by monitoring the UA solution in the concentration range from 0.01 to 65 μM. Figure 6A shows the plot of frequency response versus UA concentration. Over the low concentration range (0.04-45 μM), good linearity was obtained, as illustrated in Figure 6B. The linear regression equation was y(Hz) = 10.41–28.45[UA] μM, R = 0.9952, n = 7. The detection limit of the UA biosensor was estimated to be about 0.01 μM (S/N = 3). It was obvious that MIT/TiO_2 nanoparticle/QCM electrode exhibited superior linear range and lower detection limit to UA molecules while comparing with the previously reported UA sensors (Table 1),[7-9,11,12,34,35] which guaranteed its possible applications.

TABLE 2 The recovery determination of uric acid (UA) in urine sample

UA Concentration, μM	Recovery, %	
Added	Found[a]	
0.30	0.29 ± 0.01	96.67
2.00	2.03 ± 0.08	101.50
17.00	16.67 ± 1.12	98.06
26.00	26.00 ± 1.18	100.00
35.00	35.22 ± 1.33	100.63

[a]Average of three measurements ± SD.

Anti-interference is a significant parameter of sensor for the UA determination in physiological conditions. Some potentially common compounds, such as AA, urea, glucose, GA, purine, and cytosine, may be present in samples, which is necessary to investigate the influence generated from these compounds. Figure 7 shows the frequency responses caused by UA and interferents on the imprinted and nonimprinted TiO_2 electrodes under the same experimental conditions. The MIT/TiO_2 nanoparticle/QCM electrode exhibited a higher response to template molecules compared with the NIT/TiO_2 nanoparticle/QCM electrode. According to the frequency change, the relative selectivity coefficients of MIT/TiO_2 nanoparticle/QCM electrode for UA/AA, UA/urea, UA/glucose, UA/GA, UA/purine, and UA/cytosine pairs were 3.10, 3.87, 3.65, 3.62, 2.97, and 3.50 times greater than that for NIT/TiO_2 nanoparticle/QCM electrode, respectively. It was obvious that the constructed MIT/TiO_2 nanoparticle/QCM electrode remarkably reduced the influence of possible interferents and presented excellent selectivity and reliability towards UA determination.

The reusability of the same UA biosensor was evaluated by measuring the response signal 15 times in a continuous manner. After each injection of UA solution and the attainment of equilibrium, the UA biosensor was recovered by calcination treatment until the frequency of QCM reached a steady value. The obtained results demonstrated that the UA biosensor could be used repeatedly, and the response signal decreased by only 1.8% at the 15th cycle. The storage stability of the UA biosensor was also investigated. The sensor was stored at room temperature for 6 months and taken out for measurements of UA at the same condition per month. The sensor retained above 96% of the original frequency response after 6 months, demonstrating the high stability for UA sensing.

Urine sample was selected as the real sample to investigate the practical applicability of constructed biosensor for the determination of UA using the standard addition method. The urine sample was diluted 1000 times with 0.01-mM PBS (pH 7.4) before measurement, and no other pretreatment process was performed. The UA concentration in the urine sample determined by the biosensor was 0.39 μM. The workability of constructed biosensor was confirmed from the obtained recovery in the range of 96.67% to 101.50% (Table 2), guaranteeing the routine analysis of UA in real biological samples.

4 | CONCLUSIONS

The MIT was prepared by molecular imprinting and surface sol-gel technique. By using the MIT layer as the recognition material, a novel UA piezoelectric biosensor was fabricated by a convenient attachment of MIT on TiO_2 nanoparticle modified QCM electrode. The constructed biosensor exhibited good reproducibility, short response time, wide linear range (0.04-45 μM), low detection limit (0.01 μM), and high sensitivity and selectivity. Detection of UA in urine sample was also performed with satisfactory results.

ACKNOWLEDGMENTS

This work was supported by Program for Science&Technology Innovation Talents in Universities of Henan Province (18HASTIT007), Natural Science Foundation of Henan Province of China (182300410201 and 182300410202), Key Research Project of Henan Province (162102210223), the Key Foundation of He′nan Educational Committee (18A150029), and Doctoral Foundation Henan Polytechnic University, China (B2016-08).

CONFLICT OF INTEREST

The authors declare no conflict of interest.

AUTHOR CONTRIBUTIONS

All authors have read and approved the final manuscript. Z.C., Q.T., and X.Z. performed the research. Y.Z. and X.Z. designed the research. Z.C., Q.T., and X.Z. analyzed the data. Z.C. and Y.Z. wrote the paper.

ORCID

Zhengpeng Yang https://orcid.org/0000-0002-9086-8289

REFERENCES

1. Peng BG, Cui JW, Wang Y, et al. CeO_{2-x}/C/rGO nanocomposites derived from Ce-MOF and graphene oxide as a robust platform for highly sensitive uric acid detection. *Nanoscale*. 2018;10(4):1939-1945.
2. Dey N, Bhattacharya S. Nanomolar level detection of uric acid in blood serum and pest-infested grain samples by an amphiphilic probe. *Anal Chem*. 2017;89(19):10376-10383.
3. Sarıkaya AG, Osman B, Çam T, Denizli A. Molecularly imprinted surface plasmon resonance (SPR) sensor for uric acid determination. *Sensor Actuat B*. 2017;251:763-772.
4. Li XL, Li G, Jiang YZ, et al. Human nails metabolite analysis: a rapid and simple method for quantification of uric acid in human fingernail by high-performance liquid chromatography with UV-detection. *J Chromatogr B*. 2015;1002:394-398.
5. Saqib M, Qi LM, Hui P, et al. Development of luminol-N-hydroxyphthalimide chemiluminescence system for highly selective and sensitive detection of superoxide dismutase, uric acid and Co^{2+}. *Biosens Bioelectron*. 2018;99:519-524.
6. dos Santos PL, Katic V, Toledo KCF, Bonacin JA. Photochemical one-pot synthesis of reduced graphene oxide/Prussian blue nanocomposite for simultaneous electrochemical detection of ascorbic acid, dopamine, and uric acid. *Sensor Actuat B*. 2018;255:2437-2447.
7. Zhao DY, Yu GL, Tian KL, Xu CX. A highly sensitive and stable electrochemical sensor for simultaneous detection towards ascorbic acid, dopamine, and uric acid based on the hierarchical nanoporous PtTi alloy. *Biosens Bioelectron*. 2016;82:119-126.
8. Bai ZY, Zhou CL, Xu HB, Wang GN, Pang HJ, Ma HY. Polyoxometalates-doped Au nanoparticles and reduced graphene oxide: a new material for the detection of uric acid in urine. *Sensor Actuat B*. 2017;243:361-371.
9. Long Q, Fang AJ, Wen YQ, Li HT, Zhang YY, Yao SZ. Rapid and highly-sensitive uric acid sensing based on enzymatic catalysis-induced up conversion inner filter effect. *Biosens Bioelectron*. 2016;86:109-114.
10. Yu JH, Wang SM, Ge L, Ge SG. A novel chemiluminescence paper microfluidic biosensor based on enzymatic reaction for uric acid determination. *Biosens Bioelectron*. 2011;26(7):3284-3289.
11. Zhang CJ, Si SH, Yang ZP. A highly selective photoelectrochemical biosensor for uric acid based on core-shell Fe_3O_4@C nanoparticle and molecularly imprinted TiO_2. *Biosens Bioelectron*. 2015;65:115-120.
12. Zhao Y, Wei XY, Peng NC, Wang JH, Jiang ZD. Study of ZnS nanostructures based electrochemical and photoelectrochemical biosensors for uric acid detection. *Sensors*. 2017;17(6):1235.
13. Fang GZ, Yang YK, Zhu HD, et al. Development and application of molecularly imprinted quartz crystal microbalance sensor for rapid detection of metolcarb in foods. *Sensor Actuat B*. 2017;251:720-728.
14. Flynn KR, Martin LL, Ackland ML, Torriero AAJ. Real-time quartz crystal microbalance monitoring of free docosahexaenoic acid interactions with supported lipid bilayers. *Langmuir*. 2016;32(45):11717-11727.
15. Art JF, vander Straeten A, Dupont-Gillain CC. Immobilization of aluminum hydroxide particles on quartz crystal microbalance sensors to elucidate antigen-adjuvant interaction mechanisms in vaccines. *Anal Chem*. 2018;90(2):1168-1176.
16. Ogimoto Y, Selyanchyn R, Takahara N, Wakamatsu S, Lee SW. Detection of ammonia in human breath using quartz crystal microbalance sensors with functionalized mesoporous SiO_2 nanoparticle films. *Sensor Actuat B*. 2015;215:428-436.
17. Hao DN, Hu CX, Grant J, Glidle A, Cumming DRS. Hybrid localized surface plasmon resonance and quartz crystal microbalance sensor for label free biosensing. *Biosens Bioelectron*. 2018;100:23-27.
18. Zhang CJ, Bai WB, Yang ZP. A novel photoelectrochemical sensor for bilirubin based on porous transparent TiO_2 and molecularly imprinted polypyrrole. *Electrochim Acta*. 2016;187:451-456.
19. Chen LX, Wang XY, Lu WH, Wu XQ, Li JH. Molecular imprinting: perspectives and applications. *Chem Soc Rev*. 2016;45(8):2137-2211.
20. Xie XW, Ma XG, Guo LH, et al. Novel magnetic multi-templates molecularly imprinted polymer for selective and rapid removal and detection of alkylphenols in water. *Chem Eng J*. 2019;357:56-65.
21. Demirci G, Doğaç Yİ, Teke M. A selective molecularly imprinted polymer for immobilization of acetylcholinesterase (AChE): an active enzyme targeted and efficient method. *J Mol Recognit*. 2015;28(11):645-650.
22. Li CY, Ma XG, Zhang XJ, Wang R, Chen Y, Li ZY. Magnetic molecularly imprinted polymer nanoparticles-based solid-phase extraction coupled with gas chromatography-mass spectrometry for selective determination of trace di-(2-ethylhexyl) phthalate in water samples. *Anal Bioanal Chem*. 2016;408(27):7857-7864.

23. Li X, Ma XG, Huang RF, Xie XW, Guo LH, Zhang MY. Synthesis of a molecularly imprinted polymer on $mSiO_2@Fe_3O_4$ for the selective adsorption of atrazine. *J Sep Sci*. 2018;41(13):2837-2845.
24. Naklua WP, Suedee R, Lieberzeit PA. Dopaminergic receptor-ligand binding assays based on molecularly imprinted polymers on quartz crystal microbalance sensors. *Biosens Bioelectron*. 2016;81:117-124.
25. Eren TJ, Atar N, Yola ML, Karimi-Maleh H. A sensitive molecularly imprinted polymer based quartz crystal microbalance nanosensor for selective determination of lovastatin in red yeast rice. *Food Chem*. 2015;185:430-436.
26. Yang ZP, Liu X, Zhang CJ, Liu BZ. A high-performance nonenzymatic piezoelectric sensor based on molecularly imprinted transparent TiO_2 film for detection of urea. *Biosens Bioelectron*. 2015;74:85-90.
27. Liu MC, Ding X, Yang QW, Wang Y, Zhao GH, Yang NJ. A pM leveled photoelectrochemical sensor for microcystin-LR based on surface molecularly imprinted TiO_2@CNTs nanostructure. *J Hazard Mater*. 2017;331:309-320.
28. Kim Y, Lee KM, Chang JY. Highly luminescent tetra (biphenyl-4-yl)ethene-grafted molecularly imprinted mesoporous silica nanoparticles for fluorescent sensing of diethylstilbestrol. *Sensor Actuat B*. 2017;242:1296-1304.
29. Yang ZP, Zhang CJ. Molecularly imprinted hydroxyapatite thin film for bilirubin recognition. *Biosens Bioelectron*. 2011;29(1):167-171.
30. Yang ZP, Si SH, Zeng XM, Zhang CJ, Dai HJ. Mechanism and kinetics of apatite formation on nanocrystalline TiO_2 coatings: a quartz crystal microbalance study. *Acta Biomater*. 2008;4(3):560-568.
31. Yang ZP, Si SH, Fung YS. Bilirubin adsorption on nanocrystalline titania films. *Thin Solid Films*. 2007;515(7-8):3344-3351.
32. Zhang CJ, Luo SQ. Piezoelectric atrazine sensor based on a molecularly imprinted film of titanium dioxide. *Microchim Acta*. 2011;175(1-2):63-68.
33. Telo JP. Radicals derived from uric acid and its methyl derivatives in aqueous solution: an EPR spectroscopy and theoretical study. *Org Biomol Chem*. 2003;1(3):588-592.
34. Wang CY, Huang CW, Wei TT, Wu MY, Lin YW. Fluorescent detection of uric acid in biological samples through the inhibition of cobalt (II) catalyzed Amplex UltraRed. *Sensor Actuat B*. 2017;244:357-364.
35. Cai N, Tan L, Li Y, Xia TT, Hu TY, Su XG. Biosensing platform for the detection of uric acid based on graphene quantum dots and G-quadruplex/hemin DNAzyme. *Anal Chim Acta*. 2017;965:96-102.

How to cite this article: Zhang C, Xiao Z, Qin T, Yang Z. Modification of nanocrystalline TiO_2 coatings with molecularly imprinted TiO_2 for uric acid recognition. *J Mol Recognit*. 2018;e2775. https://doi.org/10.1002/jmr.2775